

SMALL SATELLITES ATTITUDE DETERMINATION USING A PREDICTIVE ALGORITHM FOR ATTITUDE STABILIZATION AND SPIN CONTROL

S. Marques, P. Tabuada, P. Lima

Instituto de Sistemas e Robótica
Instituto Superior Técnico
fax: +351218418291
e-mail: {sm3, pal, tabuada}@isr.ist.utl.pt

Keywords: Small satellites, attitude determination and control, extended Kalman filter, non-linear time-varying control

Abstract

This paper presents results of closed loop attitude estimation for small satellites, based on Extended Kalman filter and Singular Value Decomposition methods. The controller is based on an algorithm for attitude stabilization and spin control of small satellites using only electromagnetic actuation. Both estimators use the measurement of two sensors: magnetometer and Sun sensor. The point-by-point attitude determination methods, which include the SVD, are based on the measurements of at least two attitude sensors in a single point in time. So a problem arises when only one measurement is available. In this case, a solution to estimate the attitude until the SVD is fully operational again is presented. The control algorithm takes advantage of the time-varying nature of the problem (the geomagnetic field changes throughout the orbit) by using the most appropriate control effort (according to an energy-based criterion) given the geomagnetic field and the satellite angular velocity at each actuation instant. Results of simulations with the predictive controller in the loop for both the extended Kalman filter and the SVD attitude estimators are presented.

1 Introduction

Small satellites are nowadays an easy and inexpensive way to gain access to space and all the advantages a satellite can provide (e.g. telecommunications, environment monitoring, scientific research). Since these LEO (Low Earth Orbit) satellites have high levels of autonomy, attitude control is a key factor to support an orbit maneuver and to accomplish the satellite mission. However, due to their low budget, they suffer structure restrictions such as limited mass and volume, low cost to launch and low cost components. Usually, none of the reduced and inexpensive attitude sensors directly provides either the attitude or the angular velocity, except for Star sensors and gyros, but, even when these sensors are on-board, they are not available during the whole orbit and they often fail to work. Thus, having an efficient and reliable attitude determination algorithm feeding the controller is essential in autonomous spacecrafts such as small satellites. Satellite attitude determination methods usually fall into two classes: point-to-point and recursive estimation algorithms. Point-to-point attitude determination is based on the measurements of two or more sensors in a single point in time, while recursive estimation estimation uses information from successive time points, as well as knowledge about the spacecraft attitude dynamics model. In small satellites, only a single attitude sensor is often avail-

able, thus leading to the exploration of recursive estimation based solutions, such as the Extended Kalman Filter (EKF). The point-to-point methods are attractive for attitude estimation algorithms since the problems associated to the Kalman filter linearization or to modelling the process and observation with non-Gaussian distributions are avoided. Also, there is no need to initialize the filter or to guarantee symmetry and positive-definitive state error covariance matrix. The Singular Value Decomposition (SVD) was chosen due to its robustness and low computational requirements when considering two attitude sensors, Section 2.

In order to work properly, the attitude estimation algorithms have to face up other problems: the mathematical description of the system is non-linear, as well as the observation model [7], and the attitude representation model must be chosen appropriately. Most of the attitude representation models have advantages and disadvantages [9], but quaternion representation, $q = [q_1 \ q_2 \ q_3 \ q_4]^T$, is the most commonly used, since it is not singular for any rotation [15]. However quaternions represent a 3 dimensional rotation involving four parameters, therefore subject to the constraint $q_1^2 + q_2^2 + q_3^2 + q_4^2 = 1$, leading to difficulties in maintaining the rotation matrix orthogonality [1]. To circumvent these problems and guarantee convergence, the EKF algorithm must be modified [1], [4].

Since small satellites are typically in LEO, the preferred attitude actuators are those which generate a magnetic momentum that interacts with the Earth geomagnetic field rotating the satellite. Thus LEO satellites may be controlled strictly by geomagnetic field interaction. A magnetic moment produced by coils placed on the satellite will produce a resultant torque by interacting with the geomagnetic field, which may be used for attitude control. Nevertheless, this low power consumption approach poses several control difficulties, such as the time-dependence on the geomagnetic field along the satellite orbit and its highly non-linear mathematical description. Several researchers have explored and solved part of

the control problems posed by LEO small satellites. Ong [13] proposes some intuitive control laws to tackle this problem, but the actuation is very restricted and does not take advantage of the time-varying nature of the problem. Steyn [10] approaches the control problem by using a Fuzzy Logic Controller that achieves better results than a Linear Quadratic Regulator (LQR), despite considering the constraint of actuating on a single coil at each time. This approach suggests that a non-linear and time-varying control methodologies should be further explored so that a better problem understanding and possible solutions may be found. Wisniewski [17] compares two non-linear solutions: sliding mode control and energy based control, achieving better results than LQRs based on linear periodic theory.

In this paper, the results of the estimation algorithms comparison performed in [8] where the estimators were tested out of the control loop, are extended to closed loop using the predictive control algorithm first described in [11], and summarized in Section 3. In [11] results of applying this controller to small satellites were obtained with full attitude knowledge and no estimator in the loop. In the work reported here, the estimation algorithms EKF or SVD are feeding the predictive controller with estimates of the satellite state. A summary of the estimation algorithms and model formulation, as well as the coordinate system used throughout this work is described in Section 2. In Section 3, a description of the LEO small satellites control problem is performed and the predictive control algorithm for attitude stabilization and spin control of small satellites is summarized. The set up of the EKF and SVD algorithms are described in Section 4. The results are presented in Section 5 and obtained from a LEO small satellite simulation environment using PoSAT-1 [12] as a benchmark of the simulator.

2 Problem Formulation

2.1 Coordinate Systems

The following coordinate systems (CS) are used throughout this paper:

Orbit CS: $\{\hat{\mathbf{i}}_o, \hat{\mathbf{j}}_o, \hat{\mathbf{k}}_o\}$ -This is a right orthonormal CS whose origin is placed at the mass center of the spacecraft and attached to spacecraft orbit around the Earth. The $\hat{\mathbf{k}}_o$ is pointing zenith, $\hat{\mathbf{j}}_o$ is tangent to the orbit opposite to the orbital velocity and $\hat{\mathbf{i}}_o$ is orthogonal to the plane of orbit.

Body CS: $\{\hat{\mathbf{i}}_b, \hat{\mathbf{j}}_b, \hat{\mathbf{k}}_b\}$ - its origin is placed in the center mass of the spacecraft and its axes are the principal axes of inertia. This referential frame is attached to the body of the satellite, rotating around the axis with the smallest moment of inertia. $\hat{\mathbf{i}}_b, \hat{\mathbf{j}}_b$ and $\hat{\mathbf{k}}_b$ are aligned with the two remaining principal moments of inertia of the satellite in order to form a right-handed CS.

Control CS: $\{\hat{\mathbf{i}}_c, \hat{\mathbf{j}}_c, \hat{\mathbf{k}}_c\}$ - When the CS which origin is the satellite mass center does not include the principal axes of inertia, an additional CS must be considered which is usually denoted as the control CS. For attitude estimation purposes this issue is not taken into account since, for simplicity of the estimator algorithm, the approximation of considering the principal axes of inertia along the body CS is made, in order to increase the computational efficiency of the algorithm.

Inertial CS: $\{\hat{\mathbf{i}}_i, \hat{\mathbf{j}}_i, \hat{\mathbf{k}}_i\}$ - its origin is placed on the Earth's mass centre and it does not rotate with the Earth. The $\hat{\mathbf{k}}_i$ is along the Earth spin vector and points from South to North. $\hat{\mathbf{i}}_i$ and $\hat{\mathbf{j}}_i$ form a plane parallel to the Earth's equatorial plane, where $\hat{\mathbf{i}}_i$ is along the vernal equinox and $\hat{\mathbf{j}}_i$ complements this right-handed triad.

2.2 Attitude Dynamics

The equation of a small satellite attitude dynamics is well known and may be expressed in the Control CS as [15]:

$$I \ ^c\dot{\boldsymbol{\omega}}_{ci} = - \ ^c\boldsymbol{\omega}_{ci} \times I \ ^c\boldsymbol{\omega}_{ci} + \ ^c\mathbf{N}_{ctrl} + \ ^c\mathbf{N}_{gg} + \ ^c\mathbf{N}_{dist} \quad (1)$$

where I is the inertia tensor; $\ ^c\mathbf{N}_{ctrl}$ is the control torque; $\ ^c\mathbf{N}_{gg}$ is the gravity gradient torque; $\ ^c\mathbf{N}_{dist}$ is a disturbance torque caused by aerodynamic drag and other effects [15] and $\ ^c\boldsymbol{\omega}_{ci}$ is the angular

velocity of the Control CS w.r.t. the Inertial CS written in the control CS.

The control torque is obtained by electromagnetic interaction with the geomagnetic field [15],

$$\ ^c\mathbf{N}_{ctrl} = \ ^c\mathbf{m} \times \ ^c\mathbf{B} \quad (2)$$

where $\ ^c\mathbf{m}$ is the control magnetic moment generated by the satellite coils and will be referred as the control variable throughout this paper; $\ ^c\mathbf{B}$ is the geomagnetic field.

The kinematic equation gives the mathematical relation between the angular velocity and the derivative of the rotation vector. In this work the attitude is parameterized by quaternions. Hence, the kinematics are expressed in the Control CS as [15]

$$\frac{d}{dt}q_o^b(t) = \frac{1}{2}\Omega \left(\ ^b\boldsymbol{\omega}_{bo} \right) q_o^b \quad (3)$$

where Ω is the absolute angular velocity of a rotating frame, $\Omega \left(\ ^b\boldsymbol{\omega}_{bo} \right) =$

$$\frac{1}{2} \begin{bmatrix} 0 & \omega_z & -\omega_y & \omega_x \\ -\omega_z & 0 & \omega_x & \omega_y \\ \omega_y & -\omega_x & 0 & \omega_z \\ -\omega_x & -\omega_y & -\omega_z & 0 \end{bmatrix} \quad \text{The angular rates}$$

components are body CS w.r.t. orbit CS.

Special care must be taken when dealing with the quaternion algebra [10]. In this work, the quaternion multiplication established by Hamilton is defined by the operator \otimes [8]. Therefore, the kinematic equation becomes

$$\frac{d}{dt}q_o^b(t) = \frac{1}{2} \ ^b\boldsymbol{\omega}_{bo} \otimes q_o^b \quad (4)$$

The linearization of Equation (1) involves linearization of the attitude determination vector composed of the rotation vector and the angular velocity. Since the quaternion represents a rotation, the sum of two quaternions is no longer a quaternion, and its linearization is calculated as

$$q(t) = \delta q(t) \otimes \hat{q} \quad (5)$$

2.3 Attitude Determination Methods

Recursive methods for attitude estimation suitable for nonlinear systems, especially for a small

satellite Attitude Determination System (ADS) in closed loop, consist typically of algorithms where the linearization is performed about the filter estimate trajectory, that depends on the measurements data. Since the trajectory is continuously updated, the algorithm parameters can not be pre-computed once for the entire set of data as for batch algorithms.

The optimal state recursive estimator, in the sense that it minimizes the mean square estimation error when applied to linear dynamic systems, is the Kalman filter. Also, the Kalman filter is well suited to real-time problems because it directly estimates the state vector at a single time, based on the measurements at that time and all measurements up to that time with a fading memory. However, the Kalman filter just guarantees optimal state estimate when applied to linear systems. The state space formulation for small satellites is non-linear both regarding the system and the observation models. Still, the Kalman filter can be used by linearization of the equations that describe the system - Extended Kalman Filter (EKF) [8]. Due to this, the Kalman filter optimality and stability properties are not guaranteed. So, there are other recursive non-linear estimators, such as higher order filters, that attempt to handle inaccuracies or simplification errors resulting from the linearizations or to model the process and observation with non-Gaussian distributions [1].

A different approach to the attitude estimation problem consists on determining the attitude based on a sequence of noisy vector measurements. Given a set of $n \geq 2$ vector measurements b_1, \dots, b_n in the body system, and a set of reference vectors r_1, \dots, r_n in the orbit system, there is an orthogonal matrix A (the attitude matrix or direction-cosine matrix) that transforms rotational vectors from the orbital to the body coordinates. The problem of finding the best estimate of the A matrix was posed by Grace Wahba [14] who was the first to choose a least square criterion to define the best estimate, i.e., to find the orthogonal matrix A with determinant 1 that minimizes

the loss function

$$L(A) = \frac{1}{2} \sum_{i=1}^n w_i |\mathbf{b}_i - A\mathbf{r}_i|^2 \quad (6)$$

where w_i is a set of positive weights assigned to each measurement and $|\cdot|$ denotes the Euclidean norm. Attitude matrix A expresses orientation between the Orbital CS and Control CS and can be expressed in terms of a quaternion [15],

$$A(q) = \begin{bmatrix} q_1^2 - q_2^2 - q_3^2 + q_4^2 & 2(q_1 q_2 + q_3 q_4) & 2(q_1 q_3 - q_2 q_4) \\ 2(q_1 q_2 - q_3 q_4) & -q_1^2 + q_2^2 - q_3^2 + q_4^2 & 2(q_2 q_3 + q_1 q_4) \\ 2(q_1 q_3 + q_2 q_4) & 2(q_2 q_3 - q_1 q_4) & -q_1^2 - q_2^2 + q_3^2 + q_4^2 \end{bmatrix} \quad (7)$$

$$= (q_4^2 - \|\mathbf{q}\|^2)I_{3 \times 3} + 2\mathbf{q}\mathbf{q}^T - 2q_4[\mathbf{q} \times]$$

where $[\mathbf{q} \times]$ is a skew symmetric matrix that implements algebraically the cross product between two vectors and $\mathbf{q} = \begin{bmatrix} q_1 & q_2 & q_3 \end{bmatrix}$.

The point-to-point methods or solutions to Wahba's problem, are attractive for attitude estimation algorithms since the EKF problems are avoided and also there is no need to initialize the filter or to guarantee symmetry and positive-definite state error covariance matrix. Since the point-to-point methods are exclusively based on a set of noisy vector measurements to determine the attitude matrix, there must be two sets of measurements from different attitude sensors: magnetometers and Sun sensors.

Magnetometers are used to measure the local geomagnetic field vector (magnitude and direction). This data is compared to a model of the geomagnetic field in order to determine the attitude. Magnetometer information has the advantage of being available throughout the whole orbit as well as of low power requirements, being lightweight and inexpensive. However, it is not very accurate due to errors in the International Geomagnetic Reference Field (IGRF) models. Nevertheless, magnetometers are widely used for attitude determination as the main sensor, due to its availability. As for the Sun sensor, it reads the angle between the spin axis of the satellite and the Sun. Since the Sun is not visible during parts of the orbit due to the satellite libration or because the satellite is orbiting in the dark side of the Earth, its information is not always available.

Other sensors such as the Earth horizon sensor; Star sensor and gyroscopes are also used in LEO satellites. However Earth horizon sensors are very susceptible to errors or to fail, like Star sensors or gyroscopes. Besides, gyroscopes are not so commonly used because they are expensive for the typically small LEO satellites budget.

Among point-to-point methods (*e.g.* , Davenport's \mathbf{q} [3], the Singular Value Decomposition (SVD) method [6] was chosen in this work due to its robustness and low computational requirements when considering two attitude sensors [5].

However, problems arise when just one sensor is available, *e.g.*, when the Sun is out of range of the Sun sensor or when the satellite is in the dark side of Earth. That must be handled when the SVD is used. This will be addressed in Section 4.

3 A Predictive Control Algorithm

A new algorithm for attitude stabilization and spin control was proposed in [11] and shown to be asymptotically stable working in closed loop without an attitude determination algorithm. In this Section we will only summarize the relevant topics for the exposition in the remainder of the paper.

3.1 Problem Description

Equation (2) shows that the control torque is always perpendicular to the geomagnetic field, pointing out the non-controllability of the electromagnetic actuation. The direction parallel to the geomagnetic fields is not controllable, but the geomagnetic field changes along the orbit. This implies that, *e.g.*, yaw, is not controllable over the poles but only a quarter of orbit later, approximately over the equator. Those characteristics must be adequately explored to regulate the satellite attitude appropriately. A time-varying predictive algorithm to determine the control moment, which takes advantage of the geomagnetic field changes, is proposed as a solution to this control problem.

3.2 Motivation

Using the satellite total energy as a Lyapunov candidate function, its time derivative is given by:

$$\dot{E}_{tot} = {}^c\boldsymbol{\omega}_{co}^T {}^c\mathbf{N}_{ctrl} \quad (8)$$

where ${}^c\boldsymbol{\omega}_{co}$ is the angular velocity of the Control CS w.r.t. the Orbital CS expressed in the Control CS. The equation $\dot{E}_{tot} = 0$ represents all the control torques that lie on a plane that is perpendicular to ${}^c\boldsymbol{\omega}_{co}$. Therefore, imposing $\dot{E}_{tot} < 0$ is the same as constraining the control torque to lie "behind" the plane perpendicular to ${}^c\boldsymbol{\omega}_{co}$.

Furthermore, the control torque must always be perpendicular to the geomagnetic field. As such, the solution of this problem must satisfy two requirements:

$$\begin{cases} {}^c\boldsymbol{\omega}_{co}^T {}^c\mathbf{N}_{ctrl} < 0 \\ {}^c\mathbf{B}^T {}^c\mathbf{N}_{ctrl} = 0 \end{cases} \quad (9)$$

It can be seen from Equation (9) that, although the solution to these constraints is not a linear space, it is nevertheless an unlimited subset of a plan embedded in a three-dimensional space, in the general case, or it does not exist if ${}^c\boldsymbol{\omega}_{co}$ is parallel to ${}^c\mathbf{N}_{ctrl}$. This is equivalent to state that the solutions to this control algorithm are infinite in the general case, suggesting a control algorithm that should choose the optimum magnetic moment (or at least the best one given all the constraints) at each actuation instant to take advantage of the particular angular velocity and geomagnetic field. This approach differs from most of the others solutions available in the literature, which use a constant control law, independently of the current angular velocity and geomagnetic field.

3.3 Formulation

As in [10], the measurements of the current geomagnetic field and the satellite angular velocity are used to determine the control magnetic moment. We start by defining a cost function based

on the kinetic energy¹:

$$J = \frac{1}{2} {}^c\boldsymbol{\omega}_{co}^T \Lambda_{\Omega} {}^c\boldsymbol{\omega}_{co} \quad (10)$$

where Λ_{Ω} is a positive definite gain matrix. More insight is given, regarding the choice of the cost function, in [16].

It is also shown in [16] that it is possible to predict the effect that a given control torque will produce on the angular velocity, requiring only the knowledge of the current angular velocities and attitude, readily available from the attitude determination system. From the available magnetic moments it is possible to choose the one that minimizes the cost function (10), once the geomagnetic field value is available from the magnetometers.

4 Simulation Setup

4.1 Estimation Setup

At least one attitude sensor must be permanently available along the whole orbit for the estimator algorithm to work properly. One such sensor is the magnetometer. This made magnetometers the most used sensors for attitude determination. To avoid local measurability problems, the data from the magnetometers must be combined with other attitude sensors data (SVD algorithm) or with information from the satellite model (EKF algorithm). In the EKF approach the attitude vector is estimated by minimizing the state estimate error covariance, based on statistical assumptions concerning the uncertainties, together with a set of noisy sensor observations.

Lefferts *et. al.* [4] avoid the EKF error covariance matrix singularity, by not estimating the scalar part of the quaternion q_4 . This reduces the rank in some of the matrices involved in the algorithm, i.e., the transition matrix Φ , the error covariance matrix P and the covariance of the process Q , the Kalman gain K as well as the F matrix that con-

tains the equations of motion and the H matrix that relates sensor measurements with the state. To reconstruct the full quaternion, the fourth element of the quaternion is obtained from the estimated vector part and using the constraint $\|q\|^2 = 1$, leading to $q_4 = \sqrt{1 - q_1^2 - q_2^2 - q_3^2}$. This is the approach used in this work.

When propagating the state and covariance matrices and also to propagate the attitude quaternion, the full quaternion must be handled carefully to obtain a proper rotation. Therefore, in these steps of the algorithm, the quaternions have to be handled separately from the angular velocity. Instead of using $\frac{d}{dt}\mathbf{x}_{k+1} = \int f(\mathbf{x}(t), \mathbf{u}(t), t)dt + \mathbf{x}_k^+$, as for the angular velocity, the quaternion must be propagated through the transition matrix $\Phi = e^{\int \frac{1}{2}\Omega(w)dt}$ without approximation, resulting in $q_{k+1}^+ = \left(\cos\left(\frac{\Delta T \bar{\boldsymbol{\omega}}_k}{2}\right) \mathbf{1} + \frac{1}{\bar{\boldsymbol{\omega}}_k} \sin\left(\frac{\Delta T \bar{\boldsymbol{\omega}}_k}{2}\right) \Omega_k \right) q_k^-$, where $\bar{\boldsymbol{\omega}}_k = \sqrt{\omega_x^2 + \omega_y^2 + \omega_z^2}$ [15]. When updating the state, where the estimated state is $\hat{\mathbf{x}} = \left[\hat{\boldsymbol{\omega}} \quad \hat{\mathbf{q}} \right]^T$, the perturbation error, $\delta\hat{\mathbf{x}}_{k+1} = \left[\delta\hat{\boldsymbol{\omega}}_{k+1} \quad \delta\hat{\mathbf{q}}_{k+1} \right]$, estimated by the filter, is computed, $\delta\hat{\mathbf{x}}_{k+1} = K_{k+1} (\mathbf{y}_{meas,k+1} - A(\hat{\mathbf{q}}_k)\mathbf{y}_{orb,k})$ and in case of the angular velocity is added to the full state, $\hat{\boldsymbol{\omega}}_{k+1}^+ = \hat{\boldsymbol{\omega}}_{k+1}^- + \delta\hat{\boldsymbol{\omega}}_{k+1}$. However, to preserve the physical sense of the quaternion update, the quaternion is updated using quaternion multiplication and Equation (5),

$$\hat{q}_{k+1}^+ = \left[\sqrt{1 - |\delta\hat{\mathbf{q}}_{k+1}|^2} \right] \otimes \hat{q}_{k+1}^- \quad (11)$$

When the Sun sensor measurements are available, the measurement covariance matrix is expanded to a 6X6 matrix, $R_{tot} = \begin{bmatrix} R_{mag} & 0_{3 \times 3} \\ 0_{3 \times 3} & R_{SS} \end{bmatrix}$ and the H matrix is expanded in order to incorporate also the Sun sensor measurement, y_{SS} .

$$H_{k+1}^+ = \begin{bmatrix} 0_{3 \times 3} & \frac{\delta A(q)}{\delta q_1} & \hat{q}_{q_1} & \hat{\mathbf{y}}_{orb} \\ 0_{3 \times 3} & \frac{\delta A(q)}{\delta q_1} & \hat{q}_{q_1} & \hat{\mathbf{y}}_{SS} \\ \frac{\delta A(q)}{\delta q_2} & \hat{q}_{q_2} & \hat{\mathbf{y}}_{orb} & \frac{\delta A(q)}{\delta q_3} & \hat{q}_{q_3} & \hat{\mathbf{y}}_{orb} \\ \frac{\delta A(q)}{\delta q_2} & \hat{q}_{q_2} & \hat{\mathbf{y}}_{SS} & \frac{\delta A(q)}{\delta q_3} & \hat{q}_{q_3} & \hat{\mathbf{y}}_{SS} \end{bmatrix} \quad (12)$$

¹The use of Λ_{Ω} instead of the inertia matrix was chosen due to the possibility of defining relative weights for the angular velocities.

In the SVD approach, two attitude sensors are used (Sun sensors and magnetometers) to compute the attitude matrix without making use of the system models. When the Sun sensor measurements are not available, which happens in small periods of the orbit, the attitude dynamics equation is used to propagate the latest attitude estimates until the Sun sensor is available again and the SVD algorithm is fully operational, correcting the incurred error.

The derivative of the quaternion, from the kinematic's Equation (4), is obtained adding a pole, a , to the transfer function of the derivator system that obtains \dot{q} from q , to damp the high frequency noise. The transfer function $\frac{s}{s+a}$ is discretized using the bilinear transform, where $s \leftarrow \frac{z}{\Delta T} \frac{z-1}{z+1}$. The discrete expression to be applied between measurements with a sampling time of Δt is given by the difference equation

$$\dot{q}_{t_k} = (1-a\Delta T)\dot{q}_{t_{k-1}} - a\Delta T\dot{q}_{t_{k-2}} + q_{t_k} - q_{t_{k-1}} \quad (13)$$

Other problem with the SVD algorithm is to obtain the quaternion estimate from the attitude matrix. This can be made from Equation (7).

One of the four possible solutions is

$$\begin{aligned} \mathbf{q}_4^1 &= \pm 0.5\sqrt{1 + A_{11} + A_{22} + A_{33}} \\ q_1^1 &= 0.25(A_{23} - A_{32})/\mathbf{q}_4^1 \\ q_2^1 &= 0.25(A_{31} - A_{13})/\mathbf{q}_4^1 \\ q_3^1 &= 0.25(A_{12} - A_{21})/\mathbf{q}_4^1 \end{aligned}$$

However numerical inaccuracies may arise when \mathbf{q}_4 is very small. One way to overcome this is to compute the maximum of $\mathbf{q}_4^2 = \pm 0.5\sqrt{1 + A_{11} - A_{22} - A_{33}}$, $\mathbf{q}_4^3 = \pm 0.5\sqrt{1 - A_{11} + A_{22} - A_{33}}$, and $\mathbf{q}_4^4 = \pm 0.5\sqrt{1 - A_{11} - A_{22} + A_{33}}$ and based on this, switch among solutions [8]. The three other solutions are,

$$\begin{aligned} \mathbf{q}_1^2 &= \pm 0.5\sqrt{1 + A_{11} - A_{22} - A_{33}} \\ q_2^2 &= 0.25(A_{12} + A_{21})/\mathbf{q}_1^2 \\ q_3^2 &= 0.25(A_{13} + A_{31})/\mathbf{q}_1^2 \\ q_4^2 &= 0.25(A_{23} - A_{32})/\mathbf{q}_1^2 \end{aligned}$$

$$\begin{aligned} \mathbf{q}_2^3 &= \pm 0.5\sqrt{1 - A_{11} + A_{22} - A_{33}} \\ q_1^3 &= 0.25(A_{12} + A_{21})/\mathbf{q}_2^3 \\ q_3^3 &= 0.25(A_{23} + A_{32})/\mathbf{q}_2^3 \\ q_4^3 &= 0.25(A_{31} - A_{13})/\mathbf{q}_2^3 \end{aligned}$$

$$\begin{aligned} \mathbf{q}_3^4 &= \pm 0.5\sqrt{1 - A_{11} - A_{22} + A_{33}} \\ q_1^4 &= 0.25(A_{13} + A_{31})/\mathbf{q}_3^4 \\ q_2^4 &= 0.25(A_{23} + A_{32})/\mathbf{q}_3^4 \\ q_4^4 &= 0.25(A_{12} - A_{21})/\mathbf{q}_3^4 \end{aligned}$$

4.2 Control Setup

The control algorithm was applied to a realistic simulated model of PoSAT-1 [12]. PoSAT-1, as other satellites of the UoSAT class, has reduced control capabilities due to the values of the control magnetic moment being limited to only three different values of positive/negative polarity. Combining this restriction with the single-coil actuation, the available set of magnetic moments is reduced to only 18 different values (6 for the x coils, 6 for the y coils and 6 for the z coils).

Power consumption is another serious restriction, reflected on PoSAT-1 actuation capabilities. For each actuation on a coil there must be at least a back-off time of 100 seconds to recharge the power supplies. This means that the actuators have at most a duty cycle of 3% , since the maximum actuation time is only 3 seconds. Considering these constraints, there are only 19 available magnetic moments: the 18 already referred and the "do-nothing-solution" ${}^c\mathbf{m} = [0 \ 0 \ 0]^T$. With such a restricted search space it is not necessary to use an iterative minimization algorithm to find the optimal magnetic momentum, because all solutions can be evaluated and the best one (i.e. the one that minimizes (10)) is chosen.

5 Results

Several simulations were performed using the SimSat simulator [12] where the Predictive Controller described in Section 3 is used in closed loop with the EKF or the SVD algorithm. The

first row of Figure 1 shows a good performance attained with the predictive controller in the loop with the EKF algorithm, where γ , the angle between the local vertical and the boom axis, is reduced from 60° to less than 5° in only 3 orbits. Simulations were performed for attitude stabilization with spin control, initial conditions $\gamma = 60^\circ$, ${}^c\omega_{co} = [0.001037 \ 0 \ 0.02]^T$ and the desired reference $\gamma = 0^\circ$, ${}^c\omega_{co} = [0 \ 0 \ 0.02]^T$. The spin velocity must be kept around 0.02 rad/s due to PoSAT-1 thermal requirements. Rows 3-5 of Figure 1, show that the controller keeps the spin velocity oscillating around the reference, while the libration is being damped.

The second row of Figure 1 shows the Euler error angle, which gives the error between the estimated and the true attitude matrix. This variable tests the estimator performance. From the figure a fast convergence can be noticed, since γ is reduced in less than 1.5 orbits. To test the initial convergence of the EKF, an error of 50% was added to the initial angular velocity and to the initial Euler angles, roll, pitch and yaw. Simulation results are plotted in Figure 1 second row, showing that the EKF has a quick initial convergence. The estimator error for the angular velocity is calculated as the root mean square error (RMS),

$$E_{\omega_x} \simeq \lim_{m \rightarrow \infty} \sqrt{\frac{1}{m} \sum_{t=1}^m (\omega_x(t) - \hat{\omega}_x(t))^2} \quad (14)$$

and similiary for the E_{ω_y} and E_{ω_z} .

The estimator error for the Euler angle errors are calculated taking the RMS.

$$E_{\psi} \simeq \lim_{m \rightarrow \infty} \sqrt{\frac{1}{m} \sum_{t=1}^m (\psi(t) - \hat{\psi}(t))^2} \quad (15)$$

The other Euler angle RMS error, E_{θ} and E_{ϕ} are computed similarly.

The RMS obtained for angular velocity is: $E_{\omega_x} = 0.00109$, $E_{\omega_y} = 0.005$, $E_{\omega_z} = 0.0023$ rad/s and, for the roll - ψ , pitch - θ and yaw - ϕ angles is: $E_{\psi} = 6.32^\circ$, $E_{\theta} = 7.75^\circ$ and $E_{\phi} = 16.16^\circ$, as can be seen in Figure 1, rows 3-5.

For the SVD algorithm, in the plots of Figure 2, a signal indicating the availability of Sun sensor measurements is provided. The signal is high when measurements are available and low otherwise, originating a square wave in all plots. In Figure 2 the first row shows that the controller is converging but slower than for EKF. From the second row of Figure 2 there are orbit segments where the error of the estimates raises dramatically. This happens because the satellite is hidden from the Sun, i.e., it is "behind" the Earth. In these cases, the attitude estimation and angular velocity are obtained exclusively from propagation of the satellite attitude dynamics. This is so because the model of the Sun sensor is based on the estimates of the previous attitude which already has an error due to propagation. So the attitude obtained by the algorithm is also influenced by the error. This is also due to the angular velocity error, since, as can be seen from the kinematic equation (4), the quaternion is influenced directly by the angular velocity. The same analysis can be driven from the observation of rows 3-5 of Figure 2, where the estimates diverge from its real value. However, when the Sun is in the field of view of the sensor, the attitude estimates become closer to the true value and the error incurred by the SVD is very small when compared to the EKF results. Figure 3 details of the second row of Figure 2. If the Root Mean Square (RMS) is computed for the whole orbit, with the SVD running only when two sensors are available, the RMS errors are: $E_{\omega_x} = E_{\omega_y} = 0.00068$, $E_{\omega_z} = 0.00057$ rad/s and for the Euler angles: $E_{\psi} = 16.19^\circ$, $E_{\theta} = 9.5^\circ$ and $E_{\phi} = 17.29^\circ$. Still, the angular velocity has a very good accuracy compared with the EKF. Hence, if the RMS is only computed when SVD is running the results for the Euler angles improve considerably: $E_{\psi} \cong 0.52^\circ$, $E_{\theta} \cong 0.55^\circ$ and $E_{\phi} \cong 0.52^\circ$. Clearly, the propagation of the attitude and angular velocity through the model of the satellite is not a good option. A way to avoid this problem is to add measurements from another sensor also always available in space for small satellites: the Global Position System (GPS). Until recently, this instrument is mainly used to synchronisation and on-board or-

bit position determination. A way to improve SVD performance and to obtain a fair comparison with the EKF, as the SVD would be running the whole orbit and not just during a part of it, is to combine the magnetometers information with GPS [2].

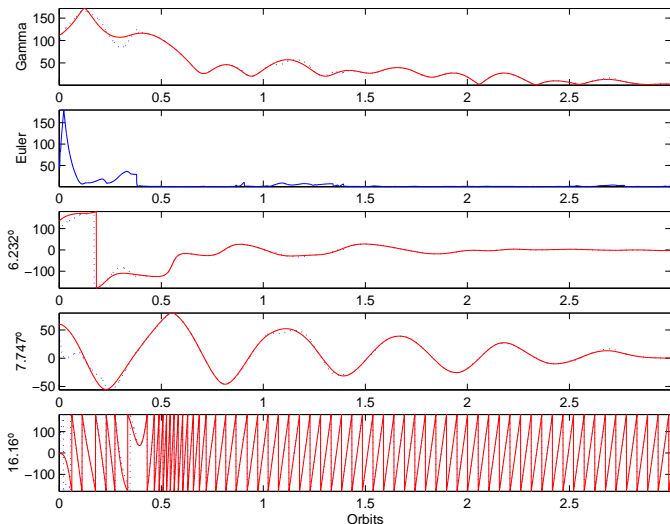


Figure 1: EKF estimator in closed loop with the predictive control algorithm. (solid line: estimation results; dotted line: true values of the variable). Row 1: γ evolution; row 2: Euler error; row 3 – 5: true and estimated angular velocity. The y-axis label of the 3rd-5th row, is the RMS for the Euler angles [roll/pitch/yaw in degrees].

6 Conclusions

In this paper we presented the results of using a predictive control algorithm for attitude control of small satellites, first introduced in [11], with an attitude estimator in the loop. Two estimators were tested: EKF and SVD. The predictive controller displayed a good performance when working in closed loop with a estimator, even when fed by attitude estimation with a large errors. Simulation results have shown that the controller works better with the EKF than with the SVD. However, the SVD deterministic method, like all point-by-point methods, computes the attitude matrix efficiently and with much less computational load than the EKF. Therefore, it is

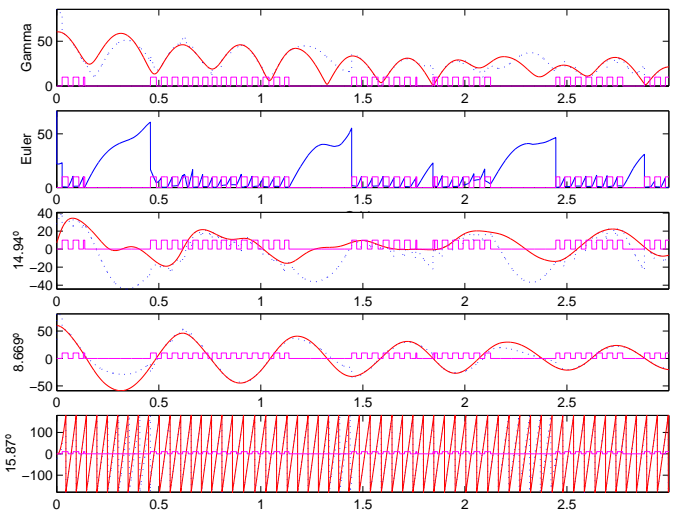


Figure 2: SVD estimator in closed loop with the predictive control algorithm. (solid line: estimation results; dotted line: true values of the variable). Row 1: γ evolution; row 2: Euler error; row 3 – 5: true and estimated angular velocity. The y-axis label of the 3rd-5th rows, is the RMS for the Euler angles [roll/pitch/yaw in degrees]. An additional signal is high when the Sun sensor measurements are available and low otherwise, originating a square wave in all plots.

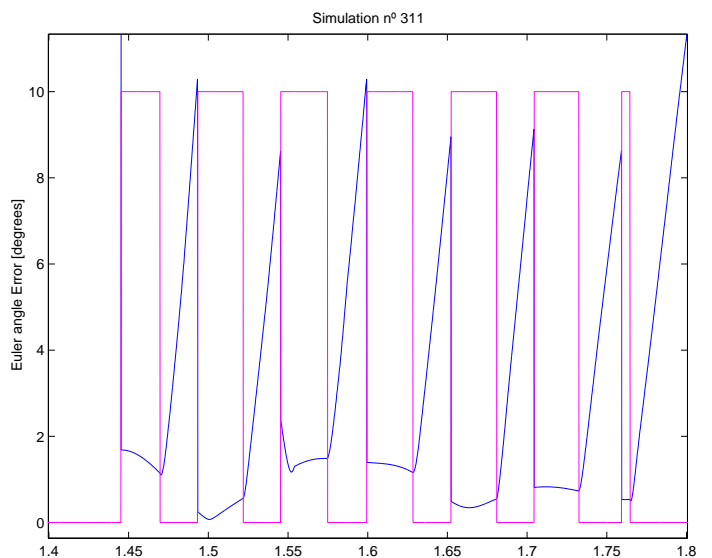


Figure 3: Euler angle error. Detail of second row of Figure 2.

attractive to implement in small satellites with short computational resources. Nevertheless, it requires two vector measurements in order to estimate the attitude. Thus, in order to have the SVD working continuously, even when just one attitude sensor is available, it was proposed to propagate the state vector through the dynamic and kinematic equations. The results obtained were not good as those obtained for the EKF but very encouraging when considering only the SVD performance. To improve the results is necessary to have two attitude sensors or to improve the computation of the estimates through the Dynamics knowledge.

References

- [1] T. Bak. "Onboard Attitude Determination for Small Satellite", *In proc.: Proceedings 3rd International Conf. on Spacecraft Guidance, Navigation and Control Systems*, ESA (1996).
- [2] J. Crassidis, F. Markley, F. Landis. "New Algorithm for Attitude Determination Using Global Positioning System Signals", *Journal of Guidance, Control and Dynamics*, **vol. 20**, No. 5, Sep-Oct. (1997).
- [3] P. Davenport. "A Vector Approach to the Algebra of Rotations with Applications", *NASA Technical Note TN D-4696*, (1968).
- [4] E. J. Lefferts, F. L. Markley, M. D. Shuster. "Kalman Filtering for Spacecraft Attitude Estimation", *Journal of Guidance, Control and Dynamics*, **vol. 5**, No 5, pp. 417-429, (1982).
- [5] F. L. Markely, D. Mortari. "How to estimate From Vector Observations", *AIAA/AAS Astrodynamics Specialist Conference*, Girdwood, Alaska (1999).
- [6] F. L. Markely. "Attitude Determination using Vector Observations and Singular Value Decomposition", *The Journal of the Astronautical Sciences*, volume 36, No. 3 (1988).
- [7] S. M Marques. "Small Satellites Attitude Determination Methods", *MSc. Thesis, IST Technical University of Lisbon*, (2001).
- [8] S. M Marques, R. Clements, P. Lima. "Comparison of Small Satellite Attitude Determination Methods", *Proc. of 2000 AIAA Conf. on Navigation, Guidance and Control*, USA (2000).
- [9] M. D. Shuster. "A Survey of Attitude Representations", *Journal of the Astronautical Sciences*, **vol. 41**, No. 4, pp. 439-517 (1993).
- [10] W. H. Steyn. "Comparison of Low-Earth-Orbit Satellite Attitude Controllers Submitted to Controlability Constraints", *Journal of Guidance, Control and Dynamics*, **vol. 17**, (1994).
- [11] P. Tabuada, P. Alves, P. Tavares, P. Lima. "A Predictive Algorithm for Attitude Stabilization and Spin Control of Small Satellites", *European Control Conf. (ECC'99)*, Karlsruhe - Germany (1999).
- [12] P. Tavares, B. Sousa, P. Lima. "A Simulator of Satellite Attitude Dynamics", *Proc. of Control'98*, 3rd Portuguese Conference on Automatic Control, **volume 2**, (1998).
- [13] W. T. Ong. "Attitude Determination and Control of Low Earth Orbit Satellites", *Msc. thesis, Dept. of Electronic and Electrical Engineering, University of Surrey*, (1992).
- [14] G. Wahba. "A Least-Squares Estimate of Satellite Attitude", *SIAM Review*, **vol. 7**, No. 3, p. 409 (problem 65-1), (1965).
- [15] J. R. Wertz. "Spacecraft Attitude Determination and Control", *Astrophysics and Space Science Library*, **vol. 73**, Kluwer Academic Publishers (1995).
- [16] R. Wisniewski., A. Astolfi, T. Bak, M. Blanke, P. Lima, K. Spindler, P. Tabuada, P. Tavares, "Satellite Attitude Control Problem", *Chapter in Control of Complex Systems (COSY)*, Springer-Verlag, Berlin (2000).
- [17] R. Wisniewski. "Satellite Attitude Control using Electromagnetic Actuation", *Ph.D. Thesis, Dept. of Control Engineering, Aalborg University* (1996).